Journal of Alloys and Compounds 489 (2010) 408–414

Contents lists available at ScienceDirect

Journal of Alloys and Compounds

journal homepage: www.elsevier.com/locate/jallcom

Diffusion and solubility of Cr in WC

M. Brieseck[a], M. Bohn[b], W. Lengauer[a,*]

[a] Institute of Chemical Technologies and Analytics, Vienna University of Technology, Getreidemarkt 9/164-CT, 1060 Vienna, Austria
[b] CNRS-UMR 6538, Centre de la Microsonde de l'Ouest, IFREMER, 29280 Plouzané, France

ARTICLE INFO

Article history:
Received 14 September 2009
Received in revised form
21 September 2009
Accepted 23 September 2009
Available online 9 October 2009

Keywords:
Chromium carbide
Tungsten carbide
Diffusion
Solubility
Hardmetal
Grain-growth inhibition
Spherical diffusion

ABSTRACT

Although no detailed study on the Cr solubility in WC exists the compilation on the various C–Cr–W phase diagrams [1] suggests this behaviour. In order to prove this and to estimate the diffusivity of Cr in WC we prepared diffusion couples of the type Cr_3C_2–WC by joining and annealing polished fully dense counterparts of the two carbides (temperature range 1550–1750 °C). After thermal treatment the diffusion couples were cut, polished and investigated by metallography. For the measurement of the diffusion profiles the couples were subjected to WDS-EPMA (Cameca SX 100 microprobe). W, Cr, and C concentration profiles were obtained from line scans performed perpendicular to the interface. The analysis of diffusion couples of WC contacted to other carbides used for doping of hardmetals (VC, TaC, NbC, and TiC) did not yield perceptible solubility of the respective metals in WC with respect to the detection limit of EPMA.

From the Cr diffusion profiles a diffusion coefficient of Cr in WC of approximately $D = 1.70–2.20 \times 10^{-11}\,cm^2/s$ and an activation energy of $E_A = 0.75\,eV$ was estimated. In addition the composition of the ternary phase $(W,Cr)_2C$ in equilibrium with WC and Cr_3C_2 could be measured. For example, in couples annealed at 1750 °C the composition reaches from $(W_{0.5}Cr_{0.5})_2C$ (in equilibrium with WC) to $(W_{0.2}Cr_{0.8})_2C$ (in equilibrium with Cr_3C_2).

With the results obtained from the analysis of diffusion couples, the Cr uptake of WC powder as a function of grain size, time and temperature was calculated. Cr saturation in idealised spherical particles of 1 μm occurs only within a few minutes.

1. Introduction

Hardmetals, widely used for cutting and drilling tools and wear resistant applications, generally consist of a high fraction of tungsten carbide (WC) grains embedded in a relatively soft and tough cobalt (Co) binder matrix. Variations in cobalt composition and the addition of cubic carbides can improve the mechanical properties [2,3]. The microstructural control with respect to size and uniformity of the carbide grains during sintering is an important issue in fabrication of hardmetals. It is well known that this goal can be approached by addition of so-called grain-growth inhibitors, like VC, Cr_3C_2, TaC, NbC or TiC, whereas VC and Cr_3C_2 are the most effective ones [4].

Hardmetal production follows a powder metallurgical route, which involves mixing of the components, granulation, pressing and sintering. To ensure effective grain-growth inhibition and uniformity of WC particles, a homogeneous distribution of grain-growth inhibitors in the powder mixture is desired. An alternative technique, capable of achieving the most uniform distribution of grain-growth inhibiting elements would consist of alloying the grain-growth inhibitors to WC. Unfortunately, WC does not perceptibly dissolve the grain-growth inhibiting carbides, possibly with one exception, Cr_3C_2. Stecher et al. [5] noted explicitly that WC does not dissolve any chromium carbide (a fact which is also contained in the collection of Upadhyaya [6]). In other studies [7,8] the Cr solubility in WC was assumed to be very low and a clear statement about this behaviour is missing. However, the ternary phase diagram collection of C–Cr–W by Villars et al. [1] suggests that a certain solubility of Cr in WC should exist, although the compilation is based on these studies [5,7,8]. An example of a C–Cr–W phase diagram indicating a small Cr solubility (circle) in WC is given in Fig. 1. For other carbides such as TiC, VC, TaC, and NbC no solubility was detected [6].

Therefore, the aim of the study reported in this paper is to prove the solubility of metals in WC and to investigate the diffusion behaviour if there is any solubility detectable. This was performed by diffusion couples, annealed at temperatures up to

* Corresponding author. Tel.: +43 1 58801 16127; fax: +43 1 58801 16490.
E-mail address: walter.lengauer@tuwien.ac.at (W. Lengauer).

0925-8388/$ – see front matter © 2009 Elsevier B.V. All rights reserved.
doi:10.1016/j.jallcom.2009.09.137

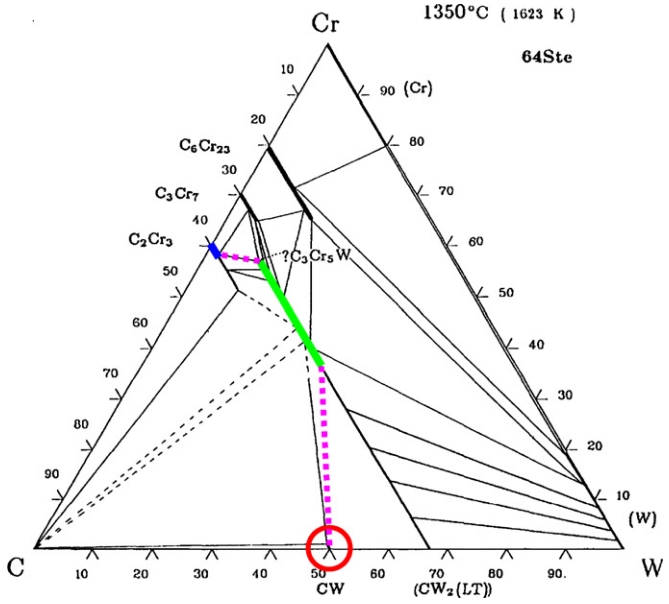

Fig. 1. Isothermal section of the W–Cr–C phase diagram at 1350 °C [1,5]. Data for T = 1750 °C for the homogeneity range of $(Cr,W)_2C$ were introduced from the present study.

1750 °C, combined with high-precision electron-probe microanalysis (WDS-EPMA).

2. Experimental

2.1. Specimen preparation

To obtain dense specimens used as counterparts for the diffusion couples, VC, Cr_3C_2, TaC, TiC, NbC, and WC powders (H.C. Starck, Germany) were compacted and sintered by hot pressing in vacuum. The oxygen partial pressure in the furnace atmosphere was not measured but was certainly very low because of the presence of graphite and graphite insolation and heating elements. Only the hot-pressed sample of Cr_3C_2 contained some larger pores which, however, was not a serious problem for further analysis. The resulting disk-like samples were cut into a final size of 10 mm × 10 mm × 10 mm. The contacting surfaces of the hot-pressed carbides were ground and polished by standard metallographic techniques up to mirror-like quality. In order to achieve identical annealing conditions all diffusion couples were sintered simultaneously in a graphite crucible at 1750 °C for 6 h under a static load of 2 kN/cm^2. For more detailed investigations in case of the Cr_3C_2–WC couples, variations in load (0–10 kN/cm^2), in annealing temperature (1550, 1650, and 1750 °C) as well as in annealing time (3, 6, 12, and 18 h) were applied. After thermal treatment the diffusion couples were cut perpendicular to the interface, ground and polished. For microstructural characterisation of the interface light optical and scanning electron microscopy were used.

2.2. Measurements of concentration profiles

Concentration profiles were measured parallel and perpendicular to the interfaces using wavelength-dispersive electron-probe microanalysis (WDS-EPMA) by means of a CAMECA SX 100 microprobe, equipped with five spectrometers and a full set of analysing crystals. Chemically characterised standards of VC, Cr_3C_2, TaC, TiC, NbC, and WC were used as a reference material for calibration [9]. Various beam conditions between 10–20 kV and 60–100 nA were adopted. Carbon (C-Kα) was measured by use of a W/Si artificial multilayer crystal with a 2d spacing of 61.254 Å. In case of the metals the crystals LLIF (for Cr-Kα, V-Kα), TAP (W-Mα, Ta-Mα), LPET (Nb-Lα), and PET (Ti-Kα) were used. The background was measured (for metals on one side of each line and combined with a slope function for calculating the background of the other side; for carbon on two sides of each line) and subtracted from the peak intensity. Typically, line scans with a step width of 1–2 μm were performed, with measurement time at each point of 10 s at the peak maximum and 5 s at the background position. For scans perpendicular to the interface at least three concentration profiles were averaged to reduce statistical errors. Some scans parallel to the interface of about 20–30 points per scan were performed in order to obtain average concentration values at some individual distances from the interface. The measured composition (in wt.%) was calculated into mol%.

3. Results and discussion

3.1. Investigation of selected diffusion couples

As an example, the microstructures near the contact interface formed at 1750 °C after an annealing time of 6 h are shown in Fig. 2a–e, where WC is always at the bottom position. The contact areas of the different carbide counterparts with WC were plane so that a perfect interface bonding could be achieved.

Cracks, resulting from stress caused by differences in thermal expansion and strain relaxing processes, propagate across the interface area and confirm that an interface reaction takes place during the annealing process. These cracks are formed only in the counterpart carbides of WC, not in WC, and stop mostly at the border to WC.

The corresponding EPMA diffusion profiles perpendicular to each bonding interface are shown in Fig. 2a–e, too. Due to restricted lateral resolution of EPMA (about 1–2 μm) some overlapping occurs and the concentration profile is not completely steep at the interface even if no mixing occurs. With exception of the Cr_3C_2–WC couple, for the counterparts with TaC, TiC, NbC, and VC no significant amount of the corresponding metal could be detected within tungsten carbide. In a depth of 1–2 μm nothing of the metal is detectable in WC. The VC–WC couple (Fig. 2a) showed formation of the $(W,V)C_{1-x}$ phase between VC_{1-x} and WC because of the solubility of W in VC and is visible in form of a narrow bright diffusion band and also in the EPMA scan, but was not further characterised in detail in this study. Possibly, also some $(V,W)_2C$ is formed.

The Cr_3C_2–WC couple (Fig. 2b) showed a wide band of $(W,Cr)_2C$ with a constant carbon profile and strongly varying W and Cr concentrations from 10.8 mol% W and 55.4 mol% Cr ([W]/[Cr] = 0.2) at the Cr_3C_2/$(W,Cr)_2C$ interface to 31.0 mol% W and 35.4 mol% Cr ([W]/[Cr] = 0.9) at the $(W,Cr)_2C$/WC interface.

The most important insight from this first screening is the fact that a significant amount of Cr was found in WC at a distance up to several microns from the interface, which is definitely not an artefact of restricted lateral resolution of EPMA. As reported by several authors [6–8] a solid solution of group IV–VI transition metal carbides in WC was not found even at much higher temperatures.

Hence, further diffusion couples of the type Cr_3C_2–WC were prepared and investigated in more detail.

3.2. Detailed investigations on Cr_3C_2–WC diffusion couple

3.2.1. Microstructure and concentration profiles

A variety of concentration profiles was measured on diffusion couples subjected to different annealing temperatures and annealing times for evaluation of the concentration of the maximum solubility c_s of Cr in WC. A maximum temperature near the decomposition temperature of Cr_3C_2 (1811 ± 10 °C [10]) was used for heat treatment processes in order to reach the maximum solubility under the boundary conditions of the applied experimental technique.

The microstructures of the Cr_3C_2–WC diffusion couples formed during the heat treatment process at 1550 °C for annealing times between 3 and 18 h are shown in Fig. 3. As mentioned above, a $(Cr,W)_2C$ subcarbide layer is formed at the interface area. This layer grows with annealing time. For example after 18 h it is twice as thick than after 3 h.

Line scans on various diffusion couples are shown in Fig. 4 and the corresponding analysis data for 1550 and 1750 °C on the Cr and W variation across the diffusion band of the subcarbide $(Cr,W)_2C$ are shown in Table 1. Due to some carbon contamination the carbon is slightly overestimated as compared to a contamination-free sam-

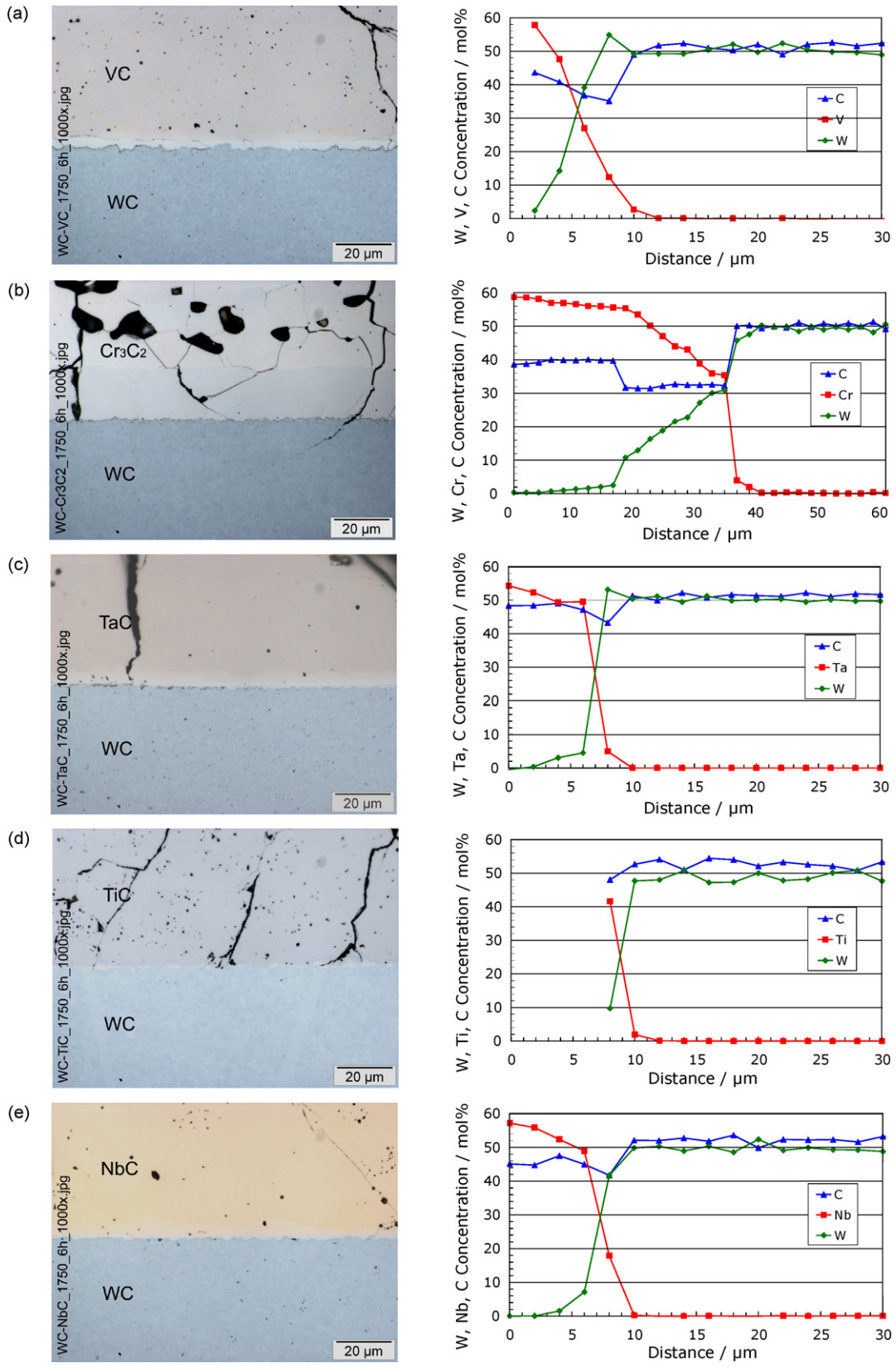

Fig. 2. Left: optical micrographs of the interface of (a) VC–WC, (b) Cr_3C_2–WC, (c) TaC–WC, (d) TiC–WC, and (e) NbC–WC diffusion couple annealed for 6 h at 1750 °C, load: 2 kN/cm^2, right: corresponding concentration profiles measured perpendicularly to the interface.

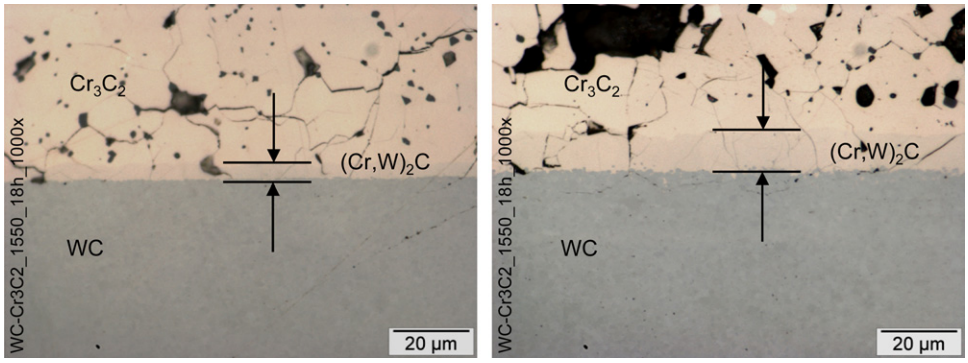

Fig. 3. Optical micrographs of the interface of Cr_3C_2–WC diffusion annealed without loading at a temperature of 1550 °C. Left: for 3 h and right: for 18 h.

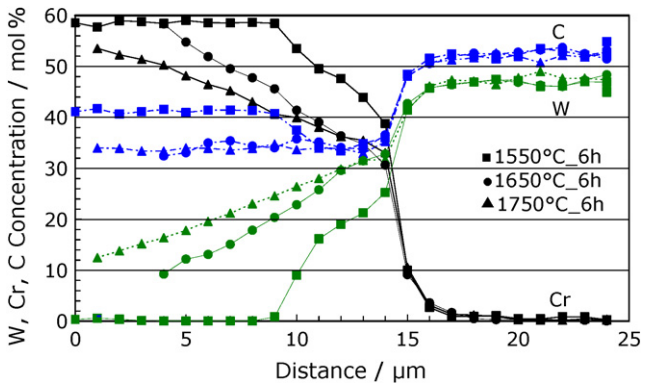

Fig. 4. Overview of measured concentration profiles starting from pure Cr_3C_2 (left) to pure WC (right) annealed for 6 h at a temperature of 1550, 1650, and 1750 °C without loading.

Table 1
Analysis data of Cr and W contents for the $(W_xCr_y)_zC$ subcarbide phase in couples annealed at 1550 and 1750 °C. Carbon is slightly overestimated due to surface C contamination as compared to Fig. 2b (z was set to 2).

Distance (µm)	$(W_xCr_y)_zC$					
	1550 °C			1750 °C		
	x	y	z	x	y	z
1				0.2	0.8	2.0
2				0.2	0.8	2.0
3				0.2	0.8	2.0
4				0.2	0.8	2.0
5				0.3	0.7	2.0
6	Cr_3C_2			0.3	0.7	2.0
7				0.3	0.7	2.0
8				0.3	0.7	2.0
9				0.4	0.6	2.0
10				0.4	0.6	2.0
11	0.2	0.8	2.0	0.4	0.6	2.0
12	0.3	0.7	2.0	0.5	0.5	2.0
13	0.3	0.7	2.0	0.5	0.5	2.0
14	0.4	0.6	2.0	0.5	0.5	2.0
15						
16	Interface/WC			Interface/WC		

ple (Fig. 2a–e). For the carbon content of the $(Cr,W)_2C$ subcarbide z was set to 2 in close correspondence to the first results (Fig. 2b). The carbon overestimation has no influence on the measured Cr content in WC.

Interestingly, in the case of long isothermal annealing and by application of a heavy static load onto the diffusion couples the plane geometry of the interface is destroyed. Fig. 5 shows an example annealed at 1750 °C for 6 h under a loading of 10 kN/cm^2. Compared to the samples presented in Fig. 2b the interface is ragged and a porous zone is formed in WC. This porous zone forms below another zone which – still located within WC – contains free $(Cr,W)_2C$ particles and is pore-free (Fig. 5, right). These phenomena are dependent on the load. The heavy external load causes plastic deformation and further Cr diffusion into WC occurs easily along destroyed grain boundaries. However, if the porosity occurring in WC is explained by the Kirkendall effect, this would be an indication that W diffuses faster into $(Cr,W)_2C$ than Cr into WC. Since neither the porosity nor the precipitation of $(Cr,W)_2C$ was found in diffusion couples at lower static loads, the porosity is probably attributed to an influence of pressure onto the microstructure of WC.

In our following investigation diffusion couples obviously affected by $(Cr,W)_2C$ precipitation and excessive void formation could not be taken into account and no additional loading was

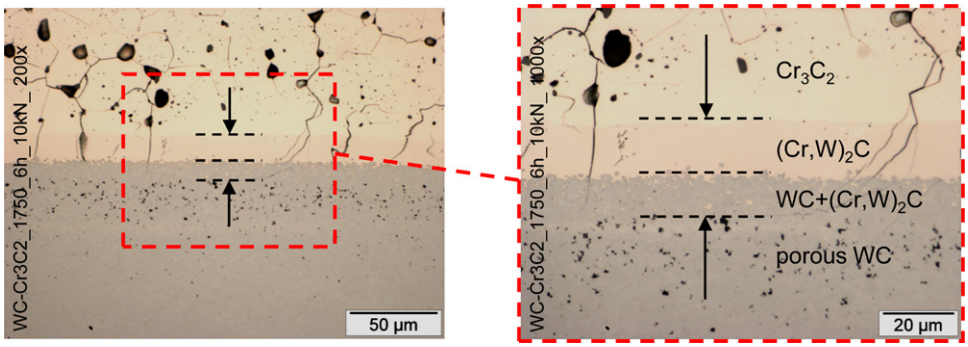

Fig. 5. Optical micrographs of the interface bonding of Cr_3C_2–WC diffusion annealed at 1750 °C for 6 h under a load of 10 kN/cm^2.

Table 2
Mean values of measured concentration profiles for different temperatures and annealing times (standard deviation given in parentheses).

	Distance (μm)	3 h		6 h		12 h		18 h	
		Mol%	Wt.%	Mol%	Wt.%	Mol%	Wt.%	Mol%	Wt.%
1550 °C	4	0.84 (0.38)	0.48 (0.21)	0.99 (0.41)	0.56 (0.24)	0.88 (0.28)	0.49 (0.16)	0.87 (0.51)	0.48 (0.29)
	6	0.55 (0.32)	0.31 (0.18)	0.66 (0.14)	0.37 (0.08)	0.74 (0.71)	0.42 (0.41)	0.80 (0.58)	0.43 (0.32)
	9	0.57 (0.37)	0.32 (0.21)	0.46 (0.29)	0.26 (0.16)	0.51 (0.40)	0.28 (0.23)	0.57 (0.12)	0.31 (0.06)
	12	0.30 (0.12)	0.17 (0.07)	0.34 (0.20)	0.19 (0.11)	0.36 (0.07)	0.20 (0.04)	0.34 (0.21)	0.19 (0.12)
	16	0.20 (0.17)	0.11 (0.10)	0.11 (0.01)	0.06 (0.01)	0.26 (0.20)	0.14 (0.11)	0.10 (0.12)	0.06 (0.07)
	20	0.11 (0.20)	0.06 (0.11)	–	–	0.25 (0.15)	0.14 (0.08)	0.21 (0.09)	0.11 (0.05)
	22	0.09 (0.09)	0.05 (0.05)	–	–	0.15 (0.06)	0.08 (0.03)	0.27 (0.12)	0.15 (0.06)
1650 °C	4	–	–	0.72 (0.43)	0.41 (0.25)	0.75 (0.32)	0.47 (0.19)	1.03 (0.61)	0.60 (0.36)
	6	–	–	0.58 (0.34)	0.33 (0.20)	1.05 (0.52)	0.75 (0.11)	0.96 (0.71)	0.56 (0.41)
	9	–	–	0.41 (0.25)	0.23 (0.14)	0.54 (0.40)	0.35 (0.25)	0.41 (0.15)	0.23 (0.08)
	12	–	–	0.21 (0.14)	0.12 (0.08)	0.40 (0.18)	0.26 (0.08)	0.41 (0.20)	0.23 (0.11)
	16	–	–	0.21 (0.11)	0.12 (0.06)	0.05 (0.05)	0.02 (0.03)	0.30 (0.09)	0.17 (0.05)
	20	–	–	0.11 (0.11)	0.06 (0.06)	0.19 (0.14)	0.12 (0.09)	0.27 (0.07)	0.15 (0.04)
	22	–	–	0.09 (0.06)	0.05 (0.03)	0.26 (0.25)	0.19 (0.13)	0.26 (0.15)	0.15 (0.08)
1750 °C	4	–	–	0.98 (0.44)	0.56 (0.26)	–	–	–	–
	6	–	–	0.73 (0.66)	0.41 (0.37)	–	–	–	–
	9	–	–	0.62 (0.58)	0.36 (0.34)	–	–	–	–
	12	–	–	0.45 (0.37)	0.26 (0.22)	–	–	–	–
	16	–	–	0.16 (0.12)	0.09 (0.07)	–	–	–	–
	20	–	–	0.23 (0.22)	0.12 (0.12)	–	–	–	–
	22	–	–	0.15 (0.06)	0.08 (0.04)	–	–	–	–

applied. For each specimen several concentration profiles were measured in WC near the $(Cr,W)_2C$–WC interface. In general, for each annealing condition at least 3 line scans perpendicular to the interface were superimposed and averaged to obtain mean concentration data. A comparison of four such line scans on samples annealed at 1550 °C for different length of time is presented in Fig. 6. It shows that an increase in annealing time leads only to a small increase of the penetration depth, an indication of the low diffusivity of Cr in WC. Due to the lateral resolution of EPMA the position of the interface is accurate to ±1 μm. The maximum solubility c_s of Cr in WC is 0.8–1.5 mol%. This solubility did not change significantly in the investigated temperature interval due to restricted precision of EPMA. Table 2 summarises the mean values of concentration profiles under different annealing conditions. For estimating the accuracy of measurement data the standard deviation is given in parentheses.

3.2.2. Estimation of the diffusion coefficient and activation energy

Assuming a concentration-independent diffusivity (based on the Fick's first law), the diffusion coefficient D was evaluated by fitting Eq. (1) to the measured data described by Crank [11] and Jost [12]:

$$\frac{c_x - c_0}{c_s - c_0} = 1 - erf\left(\frac{X}{2\sqrt{D \cdot t}}\right) \quad (1)$$

where c_0 and c_s are the initial and surface concentration (c_s is also the maximum solubility), c_x the concentration at distance x from the interface position and t the annealing time. Within the accuracy of the analytical method c_s does not change with temperature in the investigated range, compare Fig. 6 (for thermodynamic reasons increase of c_s with temperature is to be expected).

The diffusion coefficients calculated for diffusion of Cr in WC in the temperature range between 1550 and 1750 °C are summarised in Table 3. As shown in Fig. 6 the maximum solubility of Cr in WC is approximately 1.5 mol%. To omit the possible influence of the boundary the calculations were done with values of ≤1.0 mol% Cr. The data show a linear relationship between $\ln D$ and $1/T$ (Fig. 7) and hence, the pre-exponential factor D_0 and the activation energy E_A could be calculated as defined by the Arrhenius relationship (Eq. (2)), where R is the gas constant.

$$D = D_0 \exp^{-E_A/RT} \quad (2)$$

The calculated diffusion coefficient shows a low temperature dependency which results in a comparatively low activation energy of diffusion. As reported in literature activation energies for metal diffusion should be substantially larger. An example is given by Klotsman et al. [13] where diffusion of chromium and

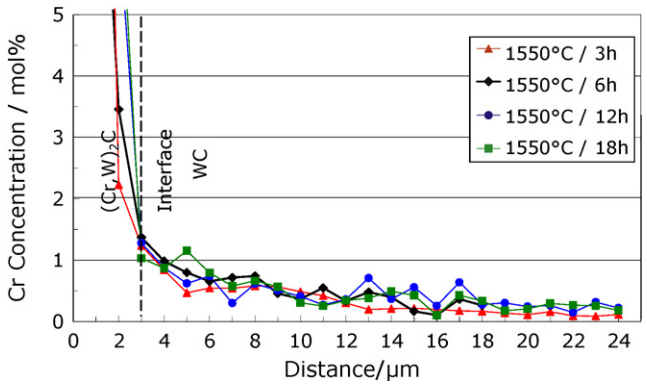

Fig. 6. Overview of measured concentration profiles (average values) of Cr_3C_2–WC couples annealed at 1550 °C for 3, 6, 12, and 18 h, without load.

Table 3
Diffusion coefficients of Cr in WC obtained from various concentration profiles measured in Cr_3C_2–WC diffusion couples annealed at different temperatures and for different times.

	Diffusion coefficient, D(cm^2 s^{-1})			
	3 h	6 h	12 h	18 h
Annealing temperature				
1550 °C	3.40E−11	1.50E−11	1.10E−11	8.10E−12
1650 °C	–	1.60E−11	1.40E−11	1.10E−11
1750 °C	–	2.20E−11	–	–
Activation energy				
E_A (kJ/mol)	–	58.00	70.30	89.21
E_A (eV)	–	0.60	0.73	0.92
D_0 (cm^2/s)	–	6.60E−10	1.10E−09	2.90E−09

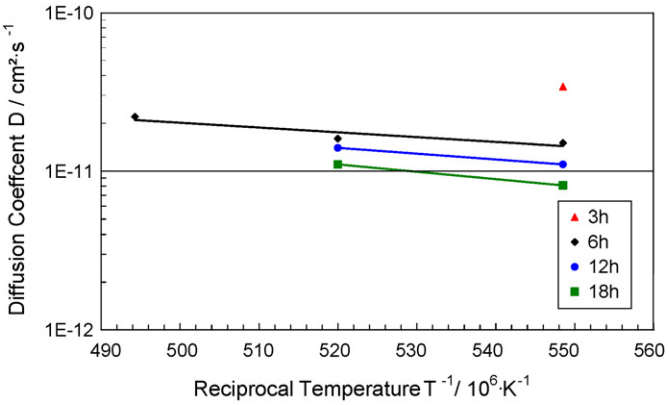

Fig. 7. Arrhenius plot for Cr_3C_2–WC couples annealed for 3, 6, 12, and 18 h.

molybdenum in tungsten single crystals was investigated. The diffusion coefficient for Cr in W was 1.81×10^{-14} cm^2/s at 1812 °C and 1.6×10^{-11} cm^2/s at 2385 °C, respectively, with an activation energy of 130.73 ± 0.52 kcal/mol (5.7 eV).

However, the low activation energy is compensated by a very low D_0 so that the complete set of data is capable of estimating diffusion of Cr in WC. Such estimation is done in the next section for the Cr uptake of WC powders, assumed as ideal spherical particles.

3.2.3. Estimation of Cr uptake into WC powder

Under the aspect of a possible Cr alloying of WC powder it was interesting to estimate the compositional change of WC powder particles. For this procedure the diffusion coefficient as well as maximum solubility of Cr in WC estimated from the above analysis of diffusion couples could be taken. A formula for the average compositional change of spheres at isothermal conditions is available in Crank [12], Eq. (3):

$$c_{av} = c_{bulk} + (c_s - c_{bulk}) \times \left[1 - \frac{6}{\pi^2} \times \sum_{n=1}^{n=\infty} \frac{1}{n^2} \exp\left(-n^2\pi^2 D \frac{t}{r^2}\right)\right] \quad (3)$$

where, for the present case, c_{av} is the average composition of Cr in a WC particle of radius r, D is the diffusion coefficient of Cr in WC, t is the time and c_s is the value for maximum solubility of Cr in WC (c_{bulk} = 0 if WC does not contain Cr previous to diffusional treatment). A calculation for different particle sizes and temperatures is shown in Fig. 8. Depending on annealing condition the time necessary for almost complete Cr uptake (c_{av} close to c_s) varies from approximately 10 min for particle diameters of 1 μm, to several 1000 min for particles exceeding diameters of 2 μm. Within the temperature range investigated the temperature influence is not as great as the influence of particle size in the range of 1–5 μm. These results show that very fine WC powders of less than 1 μm could be Cr saturated only within minutes. Because of three-dimensional diffusion the concentration change of spheres is much faster than in the one-dimensional case of planar diffusion couples, a phenomenon which is important in powder synthesis [14]. These short diffusion times allow a technical alloying procedure of WC powders with Cr up to approximately 1.5 mol% Cr.

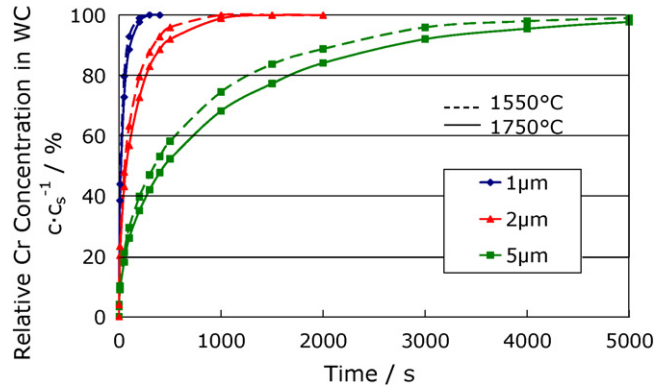

Fig. 8. Average concentration of Cr (relative to the maximum average concentration of 1.5 mol%) in WC particles as a function of annealing time at temperatures of 1550 and 1750 °C and particle size. Calculation was done for WC spheres in diameters of 1, 2, and 5 μm (Eq. (3)).

4. Conclusion

Grain-growth inhibition and microstructural design in WC–Co hardmetals by addition of various carbides is an important issue. A solid solution of various metals with WC, rather than a mixture of individual carbides, would represent the best procedure for the desired homogeneous distribution of grain-growth inhibitors.

Therefore, we studied possible metal solubilities and diffusivities in WC by means of diffusion couples of WC intimately contacted to TiC, VC, NbC, TaC and Cr_3C_2, respectively, at a temperature of 1550–1750 °C. While for TiC, VC, NbC and TaC no solubility of their metal component in WC could be detected within the limits of the applied WDS-EPMA technique, a Cr solubility was found and a more detailed study also on the diffusivity of Cr was performed in the following. According to the diffusion profiles the maximum solubility of Cr in WC is approximately 1.5 mol% and the diffusion coefficient of Cr in WC is $D = 1.5–2.2 \times 10^{-11}$ cm^2/s in the investigated temperature range. Although the accuracy of the data is certainly restricted due to the principal physical limits of the applied analytical technique we should state that to our knowledge this is the first detailed study on solubility and diffusion of Cr in WC. As a side result the homogeneity region of the subcarbide $(Cr,W)_2C$ was measured and reached, depending on annealing conditions, from $(W_{0.5}Cr_{0.5})_2C$ (in equilibrium with WC) to $(W_{0.2}Cr_{0.8})_2C$ (in equilibrium with Cr_3C_2).

The estimated diffusion coefficient of Cr as well as the maximum Cr solubility in WC was used to estimate the Cr uptake of WC powders. Calculations for spherical WC particles with a diameter of 1–2 μm show that the maximum solubility of Cr can be attained within 10–1000 min, respectively. Of course finer powders react even faster. This could facilitate the preparation of Cr-alloyed WC powders for a better microstructural design of WC–Co hardmetals.

Acknowledgement

The authors would to thank Dr. G. Gille and Mr. I. Hünsche of H.C. Starck GmbH, Goslar (Germany) for supporting this work.

References

[1] P. Villars, A. Prince, H. Okamoto, Handbook of Ternary Alloy Phase Diagrams, 5/6, ASM International, 1995.
[2] G. Gille, B. Szesny, K. Dreyer, H. van den Berg, J. Schmidt, T. Gestrich, G. Leitner, Int. J. Ref. Met. Hard Mater. 20 (2002) 3–22.
[3] W. Lengauer, R. Hochenauer, Tagungsband des Hagener Symposium 2006—Pulvermetallurgie in Wissenschaft und Praxis 22 (2006) 297–333.
[4] K. Hayashi, Y. Fuke, H. Suzuki, J. Jpn. Soc. Powder Powder Metall. 19 (1972) 67–71.
[5] P. Stecher, F. Benesovsky, H. Nowotny, Planseeberichte für Pulvermetallurgie 12 (1964) 89–95.
[6] G.S. Upadhyaya, Cemented Tungsten Carbides—Production, Properties and Testing, William Andrew Publishing, Noyes, 1998.
[7] E. Rudy, Y.A. Chang, Plansee Proceedings—Metalle für die Raumfahrt, 5th Plansee Seminar, Metallwerk Plansee AG Reutte/Tirol, 1965, pp. 786–822.

[8] E.I. Gladyshevskiy, V.S. Telegus, T.F. Fedorov, Yu.B. Kuz'ma, Metally 1 (1967) 97–100.
[9] W. Lengauer, J. Bauer, M. Bohn, H. Wiesenberger, P. Ettmayer, Mikrochim. Acta 126 (1997) 279–288.
[10] T.B. Massalski, Binary Alloy Phase Diagrams, second edition, ASM International, 1990.
[11] J. Crank, The Mathematics of Diffusion, second edition, Oxford University Press, 1975.
[12] W. Jost, Diffusion, Academic Press, New York, 1953.
[13] S.M. Klotsman, V.M. Kokloskov, S.V. Osetrov, I.P. Polikarpova, G.N. Tatarinova, A.N. Timofeyev, Phys. Met. Metall. 67 (4) (1989) 136–143.
[14] W. Lengauer, J. Phys. Chem. Solids 52 (2) (1991) 393–399.